Applied Catalysis B: Environmental 179 (2015) 44–53

Contents lists available at ScienceDirect

Applied Catalysis B: Environmental

journal homepage: www.elsevier.com/locate/apcatb

Pd–Pt catalysts on mesoporous SiO_2–Al_2O_3 with superior activity for HDS of 4,6-dimethyldibenzothiophene: Effect of metal loading and support composition

Zdeněk Vít[a,*], Daniela Gulková[a], Luděk Kaluža[a], Jaroslav Kupčík[b]

[a] Institute of Chemical Process Fundamentals of the ASCR, v.v.i., Rozvojová 135, 165 02 Prague, Czech Republic
[b] Institute of Inorganic Chemistry of the ASCR, v.v.i., Husinec-Řež 1001, 250 68 Řež, Czech Republic

ARTICLE INFO

Article history:
Received 28 January 2015
Received in revised form 23 April 2015
Accepted 30 April 2015
Available online 2 May 2015

Keywords:
Pd–Pt catalyst
Mesoporous silica–alumina
Deep hydrodesulfurization
4,6-DMDBT

ABSTRACT

Mesoporous silica–aluminas (MSA) containing 2–13 wt.% Al_2O_3 were studied as supports of Pd–Pt catalysts with total metal content 0.10–1.50 wt.%. Transformation of 4,6-dimethyldibenzothiophene (4,6-DMDBT) was evaluated both on the MSA supports and Pd–Pt/MSA catalysts in a flow reactor in the gas phase at 300 °C and 5 MPa. The catalysts were characterized by nitrogen adsorption, hydrogen chemisorption, cumene cracking activity for Brønsted acidity and some by electron probe microanalysis (EPMA) and transmission electron microscopy/energy dispersive X-ray spectroscopy (TEM/EDS). It was found that isomerization and disproportionation of 4,6-DMDBT occur on MSA supports and increase with the Al_2O_3 content. This Al_2O_3 phase had multiple effect on the properties of Pd–Pt catalysts. It controlled their Brønsted acidity and the amount of deposited active metal phase, both these factors consequently influenced the overall HDS activity and HYD/cracking selectivity. HDS on Pd–Pt catalysts proceeded almost exclusively by the hydrogenation (HYD) route and increased with the metal loading. Activities of majority of Pd–Pt catalysts correlated with their Brønsted acidities while not with metal dispersion. Pd–Pt/MSA catalysts were much more active than a conventional sulfide catalyst; the lowest metal loadings around 0.10 wt.% gave still 5–7 time more active catalysts than $CoMo/Al_2O_3$. We believe this was achieved due to the ability of mesoporous acidic supports to transform 4,6-DMDBT to more reactive compounds in cooperation with highly active Pd–Pt phase in the following HYD and HDS steps.

1. Introduction

Increasing demands on the quality of diesel fuels forces producers to decrease the sulfur content to ppm level. Residual sulfur compounds remaining after hydrodesulfurization (HDS) on conventional sulfide catalysts are mainly alkyldibenzothiophenes. 4,6-Dimethyldibenzothiophene (4,6-DMDBT) belongs to the most refractory compounds because of the rigid planar molecule with S atom hindered by adjacent methyl groups. Some attempts to increase its reactivity consisted in the addition of zeolites or amorphous silica–alumina (ASA) to CoMo (NiMo)/Al_2O_3 [1–3]. Or alternatively, to pass the feed through a zeolite containing bed at first and then through $CoMo/Al_2O_3$ in two-stage procedure [4]. In these studies, the acidic components transformed 4,6-DMDBT in more reactive compounds by isomerization (mainly 3,6-DMDBT) and dealkylation (4-MDBT) which improved the rate of HDS. Additional way to increase the 4,6-DMDBT reactivity is the hydrogenation of one aromatic ring because this allows more flexibility and reduces in this way the steric hindrance of the methyl group [5]. Some noble metals possess excellent hydrogenation properties, favorably in combination with proper supports. ASA and ultra-stable Y zeolite (USY) supported Pd, Pt and Pd–Pt catalysts have been studied as potential candidates for deep HDS with 4-ethyl,6-methyldibenzothiophene and 4,6-DMDBT [6–8]. In these studies, bimetallic catalysts were always more active than Pd ones. It is widely accepted that strong Brønsted acidity of these supports increases the electron-deficient character of the metal particles and their tolerance to S poisoning. This tolerance was higher for Pd–Pt catalysts as compared to monometallic Pd and Pt catalysts [8]. More recent studies showed that the mesoporous zeolites allow better access for larger reacting molecules such as 4,6-DMDBT. Pd, Pt and Pd–Pt supported on mesoporous Na-ZSM-5 gave in HDS of this compound substantially more active catalysts in comparison to those prepared from Na-ZSM-5 [9]. Moreover, comparison of the Pt

* Corresponding author. Tel.: +420 220 390 284; fax: + 420 220 920 661.
E-mail address: vit@icpf.cas.cz (Z. Vít).

http://dx.doi.org/10.1016/j.apcatb.2015.04.057
0926-3373/

catalysts prepared from mesoporous NaH-ZSM-5, NaH-ZSM-5 and Al_2O_3 of the known Pt dispersions led to conclusion that mesoporosity and acidity influenced HDS more than metal dispersion [10]. Positive effects of mesoporosity and Brønsted acidity were also observed with Pd catalysts prepared from mesoporous zeolites Y, Beta and ZSM-5 [11] and mesoporous USY [12].

Recently, we have synthesized mesoporous silica–alumina (MSA) containing 50 wt.% Al_2O_3 by cogelification from simple inorganic salts [13]. This material, showing proper textural properties, good thermal stability and hardness, was later employed as support of Pt catalysts in HDS of simple model compounds like thiophene (TH) and benzothiophene (BT) [14]. For this purpose, the composition of MSA was modified by post-synthesis nitric acid extraction in order to increase the acidity of support. The Al_2O_3 content was progressively diminished to 11 wt.%, which removed the non-acidic octahedral Al form and exposed the fraction of tetrahedral Al species. As a consequence, this change led to the samples with stronger Brønsted acidity and considerably higher surface area. The Pt catalysts prepared from the modified supports showed substantially improved HDS activities. Similar approach was then applied to Pd and Pd–Pt catalysts, prepared from different metal precursors and newly synthesized batches of MSA supports [15,16]. Also in these cases, the extraction of MSA greatly improved the activities of Pd catalysts in reactions of TH and BT. It was therefore interesting to find if the modified MSA supports could be considered for reaction of more bulky S molecule such as 4,6-DMDBT. At the same time, we attempted for a very low metal loading preferably less than 0.5 wt.%, which level has been up to now used as the lowest for the purpose of 4,6-DMDBT HDS [7,9,10]. However, in order to see general trends we studied the broader range of the metal loading up to 1.5 wt.%.

The aim of this work was to evaluate the suitability of MSA as the supports of Pd–Pt catalysts in HDS of 4,6-DMDBT. The first aim was to find a low but effective metal loading between 0.10–1.50 wt.%. This is because of the high cost of these metals and their possible lower utilization at higher loadings. The second variable studied was the composition of MSA, i.e., the amount of Al_2O_3 phase remaining after acid leaching and controlling the Brønsted acidity. The final amounts of Al_2O_3 in MSA were 2–13 wt.%, which was expected to provide the optimum range of acidities. The Pd–Pt/MSA catalysts were mostly prepared from $PdCl_2$ and H_2PtCl_6 with exception of two samples prepared from Cl-free precursors and included for comparison. Also an industrial sulfide $CoMo/Al_2O_3$ catalyst was tested in order to demonstrate the differences in HDS activity and products selectivity.

2. Experimental

2.1. Preparation of supports and catalysts

The starting MSA materials were synthesized from aqueous solutions of sodium metasilicate and aluminum nitrate by the procedure described in detail earlier and sieved to 0.16–0.315 mm particles [13]. These amorphous silica–aluminas contain 50 [13], 52 [15] and 19 wt.% Al_2O_3 and their BET surface areas were 491, 429 and 322 m^2/g, respectively. The samples with the reduced Al_2O_3 contents were prepared by leaching of these materials with 1N nitric acid in a rotary evaporator at 75 °C for 2 h. The modified supports were: MSA4 (4% Al_2O_3) prepared from MSA with 50% Al_2O_3, MSA9 and MSA13 (9 and 13% Al_2O_3) both prepared from MSA with 52% Al_2O_3 and MSA2 (2% Al_2O_3) prepared from MSA with 19% Al_2O_3. They were dried and calcined at 400 °C/2 h.

Monometallic Pd catalyst (0.92PdA-9, [15]) and bimetallic Pd–Pt catalyst (PdA–PtO, [16]) were included for comparison since recently showed high activities in HDS of thiophene and benzothiophene. They were prepared by impregnation of MSA9 with acetone solution of Pd acetate and by co-impregnation with acetone–water solution of Pd acetate + $Pt(NH_3)_4(OH)_2$, respectively, followed by reduction in H_2 at 400 °C. All other Pd–Pt catalysts were prepared by co-impregnation of MSA2, MSA4, MSA9 and MSA13 with aqueous solutions of $PdCl_2$ + H_2PtCl_6 at room temperature for 1 h. The amounts of the precursors were chosen to approach different total metal loadings 0.10–1.50 wt.%. The volume of the solutions was usually 1.5–3 ml per g of support. The slurries were evaporated to dryness in a rotary evaporator at 60 °C under vacuum. The dried catalyst precursors were first calcined in dry air at 500 °C (ramp 4 °C/min and dwell 3 h at 500 °C) and then ex-situ reduced in H_2 at 400 °C (ramp 4 °C/min and dwell 1 h at 400 °C) and stored. The catalysts were labeled by symbols like 0.10PdPt/MSA2, sequentially giving total metal content in wt.%, active phase and the support. The sulfided $CoMo/Al_2O_3$ catalyst (Shell 344, 2.4 wt.% Co, 9.2 wt.% Mo) was used as a typical HDS catalyst for comparison as in our previous studies [14,15].

2.2. Characterization of supports and catalysts

The chemical composition of supports and catalysts was determined by inductively coupled plasma-atomic absorption spectroscopy (ICP/AAS). BET surface areas and pore-size distributions of the samples degassed at 400 °C were determined by N_2 adsorption at relative pressures between 0.05 and 0.20 on an ASAP2010M instrument (Micromeritics). Pore volume (V_p) and pore diameter (D_p) were calculated using the BJH model and surface area of the mesopores (S_{meso}) was evaluated by the *t*-plot method.

The acidity of the supports and catalysts was characterized by their activity in cumene (CU) cracking, reaction catalyzed by Brønsted acid sites [17]. The conversions of CU into benzene and propylene x_{CU} were taken as simple indexes of the acidities, similarly as in our preceding studies [14,15]. The activity was evaluated with 20 mg of support (catalyst) in a flow micro-reactor with the fixed catalyst bed at 400 °C and 0.5 MPa [18]. The steady state conversions were evaluated during 3–5 h on stream. A gas chromatograph (GC) Agilent 4890D operated with FID detector and 30 m capillary DB-5 column (0.25 mm) at 115 °C.

The metal dispersion of catalysts was determined by dynamic H_2 adsorption on an apparatus equipped with thermal conductivity detector (Gow-Mac). The sample (40–80 mg) was reduced by H_2 for 1 h at 300 °C, purged by N_2 for 0.5 h at the same temperature and cooled to 22 °C in N_2. It was then titrated by 10 μl H_2 pulses till saturation. The dispersion was expressed by H/(Pd + Pt) ratios. The H/Pd and H/Pt = 1 stoichiometries were adopted according Anderson and Pratt [19].

The electron probe micro-analysis (EPMA) was performed on a SX-100 Instrument (Cameca, France). The reduced catalysts particles were mounted on epoxy discs, polished to expose their cross-section area and coated with thin layer of carbon. The *W* cathode operated at 15 keV and back-scattered electron mode was used during measurements.

Transmission electron microscopy (TEM) was performed on a JEM 3010 electron microscope (Jeol) equipped with LaB_6 cathode operating at 300 kV. Two selected samples were grounded in an agate mortar and suspended in ethanol. Droplets of the suspensions were placed on carbon film on microscopy Cu grid. Chemical composition of the deposited particles was analyzed by energy dispersive X-ray (EDS) detector (Oxford Instruments). Several images of different regions of the catalyst surface and EDS analyses of the isolated bigger particles and areas with the collections of highly dispersed metals were taken. The diameter of the analyzed areas was around 20–30 nm and the time scan 100 s.

2.3. Catalytic tests

2.3.1. HDS of 4,6-dimethyldibenzothiophene

The activity of the catalysts in HDS of 4,6-DMDBT was evaluated in the gas phase in a flow stainless steel integral reactor (i.d. 4 mm) with fixed bed of catalyst at 300 °C and 5 MPa. The feed contained 0.33 wt.% 4,6-DMDBT (97%, Aldrich), corresponding to 500 ppm S and 0.12 wt.% *n*-octadecane (99%, Alfa Aesar) as internal standard in *n*-decane (99%, Alfa Aesar). The feed rate F_{DMDBT} was in the range 0.05–0.34 $mmol_{DMDBT}/h$ and the catalyst weight W was 15–80 mg. The catalyst was diluted with α-Al_2O_3 (Alfa Aesar) to obtain a 30 mm bed followed by a 30 mm layer of glass beads facilitating preheating and stable evaporation of the feed. This was fed by a pulse-free HPLC pump into reactor. The reaction mixture was condensed in a cooled separator and the condensate was periodically drained off by a needle valve.

Before test, Pd and Pd–Pt catalysts were in situ re-activated by H_2 at 300 °C and atmospheric pressure, using a ramp 4 °C/min and a dwell 1 h at 300 °C. The CoMo catalyst was in situ re-sulfided in 10% H_2S/H_2 and atmospheric pressure at 400 °C/1 h. After activation, the input gas was switched to H_2 (200 ml/min) and the reactor temperature adjusted to 300 °C. The pressure was gradually increased to 5 MPa and the reaction started by introducing of the liquid feed. Stabilization of the reaction conditions was usually attained in 1 h and the reaction was carried out usually 3 h. The liquid samples were off-line analyzed on a gas chromatograph Agilent 4890D with a 30 m capillary DB-5 column (0.53 mm, JW Scientific) at 265 °C. These conditions allowed to separate and quantify majority of the reaction products excepting toluene and methylcyclohexane, which were analyzed separately at 230 °C. The compounds were identified by addition of the authentic standards and (or) by GC–MS analyses on a gas chromatograph HP 6890 coupled to MS detector HP 5973 (Agilent). The activities of catalysts were expressed by the first-order rate constants of 4,6-DMDBT disappearance k_{DMDBT} [7,4,20,21]. They were calculated according to equation

$$k_{DMDBT} = -\left(\frac{F_{DMDBT}}{W}\right)\ln(1 - x_{DMDBT}),$$

where F_{DMDBT}, W and x_{DMDBT} are the feed rate, weight of catalyst and the 4,6-DMDBT conversion, respectively. The selectivity was expressed as

$$S(\%) = \frac{100Y_i}{x_{DMDBT}},$$

where Y_i is the yield of compound *i*.

The content of residual sulfur in the organic compounds was determined in selected reaction mixtures by energy dispersive X-ray fluorescence (ED-XRF) on a Spectro iQII apparatus (Spectro analytical instruments). Calibration was done with thianthrene in decane in the range 0–500 ppm S. The voltage 25 keV and time period 180 s were used for individual determination. Before S determination, H_2S was blown out from the samples of reaction mixtures by N_2 (30 ml/min) at room temperature for 20 min.

2.3.2. Transformation of 4,6-DMDBT on MSA supports

Reaction of 4,6-DMDBT over MSA supports was carried out at 300 °C and 5 MPa in H_2 stream in the same catalytic setup as HDS. The amount of support was 23–35 mg and the feed rate F_{DMDBT} = 0.1 $mmol_{DMDBT}/h$. The samples were taken in 0.5 h interval and analyzed at 265 °C on the same column as the products of HDS. Molecular weights of the reaction products were evaluated by the separate analyses on a gas chromatograph HP 6890 coupled to MS detector HP 5973. The reaction was carried out 2–3 h. Major deactivation occurred on some supports so only conversions after 1 h on stream were considered.

Table 1
Properties of MSA supports.

Support	Content (wt.%)		S_{BET}	S_{meso}	D_p	V_p	x_{CU}[a]
	Al_2O_3	Na	(m^2/g)	(m^2/g)	(nm)	(cm^3/g)	
MSA2	2	0.07	385	257	3.6	0.38	0.43
MSA4	4	0.15	513	344	3.7	0.53	0.49
MSA9	9	0.01	583	417	4.0	0.66	0.76
MSA13	13	0.10	611	418	3.6	0.64	0.67

[a] Conversion of cumene cracking.

3. Results and discussion

3.1. Properties of MSA supports

Table 1 summarizes the properties of the modified MSA supports. The original content 19–52 wt.% Al_2O_3 in the synthesized materials was diminished by post-synthesis acid leaching to 2–13 wt.%. As shown in our preceding studies [14,15], this treatment removed majority of the non-acidic Al_{oct} form and enriched the Al_2O_3 phase by Al_{tet} species. The later species are associated with strongly acidic hydroxyls responsible for Brønsted acidity of ASA [22]. Together with Al_2O_3 extraction, this leaching also removed part of the residual sodium originating from sodium metasilicate used in MSA preparations. The sodium contents given in Table 1 are typical, including the value 0.01 wt.% Na, which has been achieved also in our preceding studies [14,15]. However, the individual sodium contents depend on the composition of the parent MSA (Si/Al ratio) and the extent of dealumination.

The activity of the supports in catalytic cracking of cumene (x_{CU}) decreased in the order MSA9 > MSA13 > MSA4 > MSA2, showing trend more or less parallel to their Al_2O_3 contents. The maximum activity of the MSA9 sample can be explained by much lower content of residual sodium in comparison to the other supports. These data show that MSA9 and MSA13 possess substantially higher acidities than MSA4 and MSA2.

The second positive effect of acid leaching is substantial increase of the surface area approaching up to 50%. The modified supports showed the BET values between 385–611 m^2/g and high mesoporosity; the mesopores surface area was around 70% of the BET surface area (Table 1). It seems that surface area and possibly also the pore volume are in a relation to Al_2O_3 content. On the other hand, the average pore diameter D_p did not change substantially with the support composition and remained near to 4 nm.

3.2. Properties of Pd–Pt catalysts

The composition, metal dispersion and textural properties of the catalysts after reduction are given in Table 2. The bimetallic Pd–Pt samples prepared from metal chloride precursors showed similar atomic Pd:Pt ratios around 3–4 and varying total metal loadings between 0.10 and 1.50 wt.%. The contents of residual chlorine checked in two catalysts with the highest metal loadings 1.32 and 1.50 wt.% were 0.07 and 0.09 wt.% Cl, respectively, and one can assume that their amounts were adequately lower in the remaining samples. The bimetallic PdA–PtO sample prepared from an older batch of MSA9 contained more Pt (Pd:Pt = 2) as compared to the other samples. On the other hand, the 1.50PdPt/MSA13 catalyst was more enriched by Pd (Pd:Pt = 4.6).

Almost all catalysts showed high metal dispersions irrespective of the Al_2O_3 contents and metal loadings (Table 2). The only exception was the 1.50PdPt/MSA13 catalyst showing H/(Pd + Pt) ratio 1.86. This value shows on the presence of β-Pd hydride, observed on some Pd containing samples also in our preceding studies [15,16].

Table 2
Composition, metal dispersion and textural properties of catalysts.

Catalyst	Composition (wt.%)		At. ratio	H/(Pd + Pt)	S_{BET} (m^2/g)	S_{meso} (m^2/g)	D_p (nm)	V_p(cm^3/g)
	Pd	Pt	Pd:Pt					
0.92PdA-9	0.92	0.00	–	0.86	533	373	3.8	0.59
PdA–PtO	0.38	0.35	2.0	0.68	564	399	3.7	0.60
0.10PdPt/MSA2	0.06	0.04	2.8	0.49	346	232	3.9	0.38
0.32PdPt/MSA2	0.21	0.11	3.4	0.96	358	246	3.8	0.37
0.82PdPt/MSA2	0.57	0.25	4.1	0.76	329	232	3.9	0.36
1.23PdPt/MSA2	0.84	0.39	3.9	0.95	331	233	3.8	0.35
0.11PdPt/MSA4	0.07	0.04	3.0	0.49	487	342	3.6	0.49
0.31PdPt/MSA9	0.20	0.11	3.5	0.48	484	345	4.5	0.64
0.74PdPt/MSA13	0.47	0.27	3.2	0.38	439	315	4.1	0.53
1.32PdPt/MSA13	0.83	0.49	3.1	0.78	435	328	4.4	0.57
1.50PdPt/MSA13	1.07	0.43	4.6	1.86	459	318	4.1	0.55

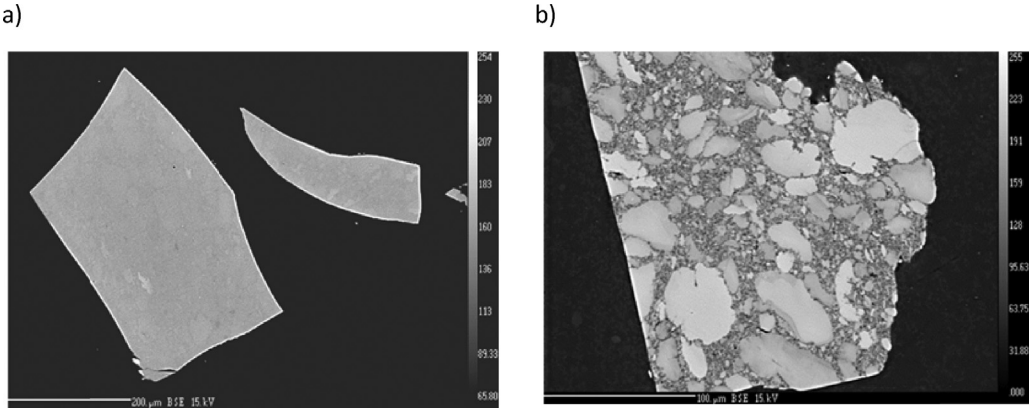

Fig. 1. Back-scattered electron EPMA images of reduced 0.10PdPt/MSA2 (a) and 0.31PdPt/MSA9 (b).

In this work, its formation was most probably facilitated by substantially lower content of Pt, which is known to prevent the β-Pd hydride formation ([23] and References therein). The results of dispersion evaluation were corroborated by the EPMA analyses of the two selected samples with relatively lower H/(Pd + Pt) values of 0.48 and 0.49. Fig. 1 shows the micrographs of the cross-sections areas of their particles. Both pattern were typical for well dispersed Pd–Pt catalysts, similarly to the pattern for PdA–PtO sample evaluated by EPMA in our previous work [16]. We conclude that some major sintering of the metallic phase in Pd–Pt/MSA can therefore be ruled out.

Additional information concerning the dispersion and composition of the metal phase was obtained by TEM/EDS. Fig. 2 shows the micrographs of two samples differing in the metal loading and HDS activity. Only few metal particles of around 3 nm were visible in the case of 0.11PdPt/MSA4, which we ascribe to a very low metal density (Fig. 2a). The EDS showed only the elements corresponding to MSA4 support while metals were not detected (not shown). Fig. 2b shows the micrograph of the 1.32PdPt/MSA13 sample, where a cluster of bigger particles and abundant fine particles of 1–3 nm are apparent. EDS of the isolated small particles failed due to their mobility under the electron beam and therefore the large scale EDS (>20 nm) of several regions rich on bigger and fine particles were carried out. The results are shown in Table 3. Some larger particles contained Pd and Pt and their bimetallic character was clearly evidenced. However, certain fraction of the bigger particles contained only Pd which shows that the alloyed Pd–Pt and Pd clusters coexist in 1.32PdPt/MSA13. This is the same result as recently obtained by Yu et al. with another Pd–Pt/ASA catalysts of similar composition and metal dispersion [24]. A rough estimate showed that the number of the bigger particles in 1.32PdPt/MSA13 was less than 3%, then absolute majority of the particles was of the size 1–3 nm. Their corresponding dispersions D should be 1.00 and 0.37 according to the equation $D = 1.12/d$, where d is particle diameter ([25] and References therein, [9]). The average value of 0.69 is not far from that of 0.78 obtained by H_2 sorption. On the other hand, there is obvious uncertainty in the composition of the fine particles. They contain only Pd according to EDS, which result, however, contradicts to global AAS analysis. The content of Pt in the metal phase of 1.32PdPt/MSA13 is $100 \times 0.49/1.32 = 37$ wt.% Pt according to AAS. However, the amount of Pt found in bigger particles by EDS corresponded to only 5 wt.% of the metal phase. This approximate value was estimated assuming a ratio of big/small particles visible by TEM in several micrographs equal to 3/97, the observed particles size and an average Pd:Pt ratio of 5 (Table 3). The missing Pt fraction is then $100\,(37 - 5)/37 = 86\%$, which must be present in highly dispersed form. The reason why majority of dispersed Pt was not found by EDS may be caused by its lower concentration and

Table 3
EDS analyses of the reduced 1.32PdPt/MSA13 catalyst.

Area	No. of particles/ size (nm)	Composition (atomic %)[a]					Ratio Pd:Pt
		C	Al	Si	Pd	Pt	
1	One/10 x 18	95.8[b]	0.2	1.8	0.55	0.15	3.7
2	One/10	0	6.3	34.6	5.29	0.87	6.1
3	One/6 x 12	0	6.1	39.2	10.9	2.09	5.2
4	One/8 x 15	0	5.7	36.2	0.90	0	–
5	One/10 x 15	0	6.2	36.2	1.12	0	–
6	Group/each ≈ 1	0	6.4	35.4	0.35	0	–
7	Group/each ≈ 1	0	5.0	47.1	0.69	0	–

[a] Contents of oxygen and Cu not shown.
[b] C originates from carbon film on a Cu grid.

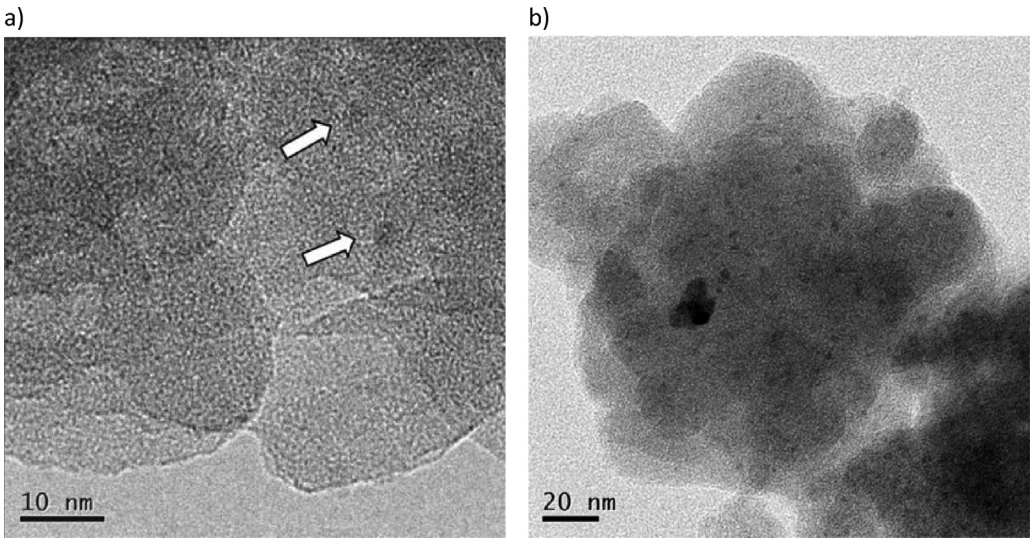

Fig. 2. TEM micrographs of reduced 0.11PdPt/MSA4 (a) and 1.32PdPt/MSA13 (b).

occlusion in the mesoporosity of MSA, similarly as was observed in the study of Pd–Pt/Beta zeolite catalysts by Roldán et al. [26].

Deposition of relatively low metal amounts on the supports with large surface areas only slightly influenced their textural properties. The adsorption–desorption isotherms of N_2 on the catalysts with different supports are shown as typical examples in Fig. 3. All isotherms are of type IV with the H2 hysteresis loop characteristic for mesoporous materials. The BET and V_p values of all catalysts are close to the values for parent supports and are given in Table 2. On the other hand, the average pore diameter D_p of Pd–Pt catalysts prepared from MSA2, MSA4 and MSA13 were little larger than those of the corresponding supports, which could be explain by partial blocking of the narrowest pores by metallic phase. Taking into account the size of the metal particles evaluated by TEM, one can ascribe this effect to highly dispersed Pd and Pt, which may enter the porosity of MSA. On the other hand, the bigger Pd and alloyed Pd–Pt particles are expected to be located at the outer surface of catalyst.

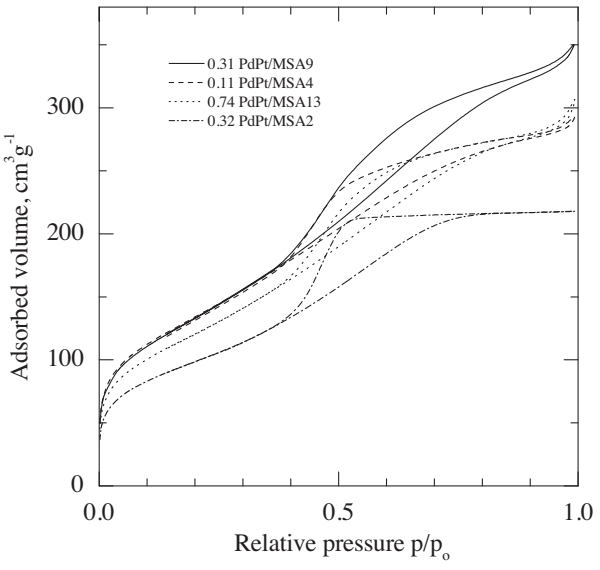

Fig. 3. Nitrogen adsorption–desorption isotherms of catalysts with different MSA supports.

3.3. Activity of MSA supports in transformation of 4,6-DMDBT

All modified MSA supports transformed 4,6-DMDBT at 300 °C by isomerization and disproportionation into several products. Isomerization led to the compound with the same molecular weight and little higher retention time as for 4,6-DMDBT. Similarly as other authors, we ascribe it to 3,6-DMDBT on the basis of the comparison of our chromatographic data with those published in the literature [2,27]. The products of disproportionation were 4-methyldibenzothiophene (4-MDBT) and trimethyldibenzothiophene (TMDBT) without further specified positions of the methyl groups. The activity and selectivity of supports in transformation of 4,6-DMDBT is given in Table 4. It is apparent, that the overall rate of transformation, expressed by the first-order rate constant of 4,6-DMDBT disappearance, k_{DMDBT}, fits fairly well the content of Al_2O_3. This finding supports the idea that this fraction of aluminum, or at least its substantial part remaining after acid leaching is the carrier of strong protonic sites capable to catalyze both reactions. However, the most acidic MSA9, according to its cumene cracking conversion x_{CU} (Table 1), was less active than MSA13. We assume that this discrepancy could be caused by a much lower sodium content in MSA9, leading to the creation of a small fraction of the strongest sites, still active in cumene cracking but easily deactivated in 4,6-DMDBT reaction. In two cases, the yields of 4,6-DMDBT transformation on MSA4 and MSA9 were distinctly lower than the x_{DMDBT} values. We ascribe these differences, denoted in Table 4 as missing products, to coke formation on acid sites. Strong deactivation was also observed by other authors during 4,6-DMDBT isomerization on a commercial ASA with 14% Al_2O_3 and explained by coke formation as a most probable reason [3]. Irrespective of this point, the experiments with the bare supports confirmed their ability to transform the refractory 4,6-DMDBT to other products. This is beneficial property for good HDS activity, because 3,6-DMDBT, 4-MDBT and some isomers of TMDBT are known as more reactive than 4,6-DMDBT due to their lower steric constraints [4].

3.4. Activity of Pd–Pt catalysts in HDS of 4,6-DMDBT

Separate experiments with the MSA supports showed that some part of 4,6-DMDBT was transformed in 3,6-DMDBT. This compound is sometimes found in smaller amounts in the reaction products of HDS [1,3,11]. We found it also in the reaction mixture after beginning of the run with 0.11PdPt/MSA4, which

Table 4
Transformation of 4,6-DMDBT on MSA supports. 300 °C/5 MPa. F_{DMDBT} = 0.1 mmol/h.

Support	W (mg)	x_{DMDBT}	k_{DMDBT} (mol/h kg$_{MSA}$)	Selectivity (%)			
				3,6-DMDBT	4-MDBT	TMDBT	Missing products
MSA2	32.8	0.02	0.06	100	0	0	0
MSA4	34.8	0.07	0.21	29	14	0	57
MSA9	34.7	0.16	0.51	31	25	6	38
MSA13	23.0	0.13	0.61	38.5	38.5	23	0

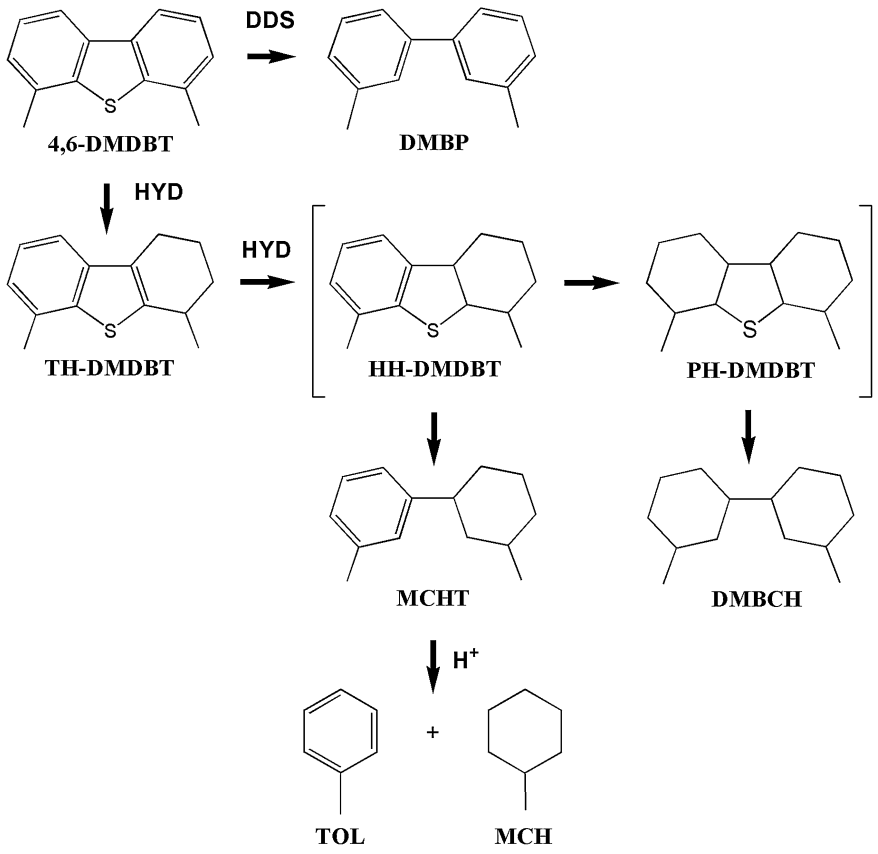

Scheme 1. Simplified reaction network of HDS of 4,6-DMDBT.

shows that isomerization occurs also on our Pd–Pt catalysts. We suppose that the following transformation of 3,6-DMDBT is the same as for 4,6-DMDBT. The main reaction network is shown in Scheme 1. This is for Pd and Pd–Pt/MSA catalysts the almost exclusive HYD route via dimethyltetrahydrodibenzothiophene (TH-DMDBT) to dimethylhexahydrodibenzothiophene (HH-DMDBT) and dimethylperhydrodibenzothiophene (PH-DMDBT), which are desulfurized in methylcyclohexyltoluene (MCHT) and dimethylbicyclohexyl (DMBCH), respectively. Cracking of MCHT gives toluene (TOL) and methylcyclohexane (MCH). Two intermediates, HH-DMDBT and PH-DMDBT were not found by us in the reaction mixtures, which can be explained by their fast transformation on noble metal catalysts [7,9]. Smaller over-stoichiometric excess of MCH can be ascribed to its simultaneous formation from TOL [12].

Basic conversion data for HDS of 4,6-DMDBT, the rate constants for 4,6-DMDBT disappearance k_{DMDBTH} and selectivity are summarized in Table 5. The first experiments were carried out with the monometallic Pd catalyst (0.92PdA-9) and Pd–Pt catalyst (PdA–PtO) prepared by us earlier from non-chlorine precursors [15,16]. Their comparison in the 4,6-DMDBT test showed that the bimetallic PdA–PtO sample, although with a lower metal loading, was substantially more active than monometallic 0.92PdA-9 catalyst. This is the same result as observed by us earlier in reactions of thiophene and benzothiophene. Higher HDS activities of Pd–Pt catalysts prepared from ASA, USY zeolite and mesoporous Na-ZSM-5 in comparison to their Pd counterparts were also observed earlier by other research groups [6–9]. Table 5 shows that the selectivity of Pd and Pd–Pt catalysts was similar, with exception of a small amount of dimethylbiphenyl (DMBP) in the products obtained with PdA–PtO. The influence of individual metals on the selectivity is seen by comparison of 0.92PdA-9 and PdA–PtO catalysts prepared from the same MSA9 support. Monometallic Pd catalyst showed considerably higher HYD activity of the aromatic ring which led to greater amount of DMBCH. On the other hand, the addition of Pt led to higher hydrogenolytic activities of the C—C and C—S bonds, giving greater amounts of cracking products (TOL, MCH) and DMBP, respectively. Higher hydrogenolytic activity of Pt is in accordance with the observations made earlier in a similar study [7]. The minor formation of DMBP by the direct desulfurization (DDS) pathway, observed exclusively on PdA–PtO, can be ascribed to separate Pt particles present in this catalyst as a consequence of the partially alloyed metal phase [16]. On the contrary, DMBP was not found in the reaction products over the remaining Pd–Pt/MSA catalysts, which supports the idea that Pt in these samples was completely alloyed with Pd.

Table 5
Activity and selectivity of catalysts in HDS of 4,6-DMDBT. 300 °C/5 MPa.

Catalyst	W (mg)	F_{DMDBT} (mmol/h)	x_{DMDBT}	k_{DMDBT} (mol/h kg_{cat})	Selectivity (%)					
					TH-DMDBT	DMBP	MCHT	TOL	MCH	DMBCH[a]
0.92PdA-9	15.6	0.136	0.76	12.3	17	0	4	3	5	71
PdA–PtO	16.0	0.136	0.89	18.5	13	2	24	9	9	43
0.10PdPt/MSA2	22.9	0.136	0.70	7.1	19	0	0	4	7	70
0.32PdPt/MSA2	17.7	0.136	0.92	19.3	3	0	8	4	9	76
0.82PdPt/MSA2	15.0	0.136	0.91	21.7	5	0	8	4	10	73
1.23PdPt/MSA2	17.5	0.17	0.91	23.2	7	0	8	3	7	75
0.11PdPt/MSA4	22.6	0.136	0.82	10.2	10	0	10	7	11	62
0.31PdPt/MSA9	43.5	0.340	0.87	15.8	2	0	7	9	11	71
0.74PdPt/MSA13	40.4	0.272	0.88	14.1	7	0	7	9	9	68
1.32PdPt/MSA13	15.4	0.204	0.90	30.3	7	0	16	3	6	68
1.50PdPt/MSA13	10.9	0.136	0.84	22.3	13	0	15	2	5	65
$CoMo/Al_2O_3$	80.4	0.068	0.83	1.5	0	27	71	1	1	0

[a] Mixture of isomers, calculated as balance.

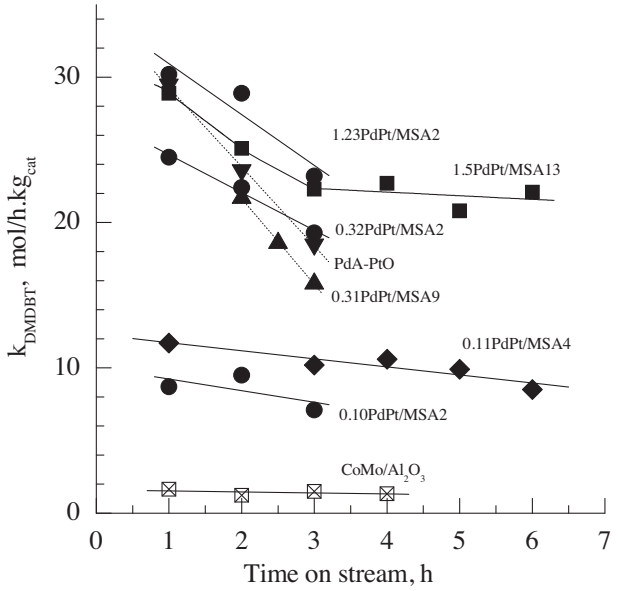

Fig. 4. First-order rate constants for 4,6-DMDBT disappearance as a function of time on stream. PdPt/MSA2 (●), PdPt/MSA4 (♦), PdA–PtO (▼), PdPt/MSA9 (▲), PdPt/MSA13(■), CoMo/Al2O3 (⊠).

The Pd–Pt/MSA catalysts showed certain decline of activities during 4,6-DMDBT catalytic tests, which is documented in Fig. 4. Such decrease can be ascribed both to sulfidation of the metal phase and coke formation on acid sites of catalysts. Data in Fig. 4 suggest that the composition of the support played the overwhelming role because the most pronounced activity decline was observed on PdA–PtO and 0.31PdPt/MSA9 samples, both prepared from the most acidic MSA9 support. Moreover, the sulfur tolerance of PdA–PtO evaluated in our preceding study [16] was close to values usually found for another PdPt/ASA and PdPt/USY zeolite catalysts [8]. We therefore propose that the coke formation is the main source of catalysts deactivation in our work. It should be noted, that deactivation of Pd–Pt/MSA catalysts in HDS of 4,6-DMDBT was much lower than that observed in isomerization with the MSA supports. We assume that hydrogen activated on the metal phase facilitates the transformation of carbonaceous deposits in volatile hydrocarbons which leads to partial recovery of acid sites and restoration of HDS activity. Activity of this series of catalysts differing in the metal loading and support composition will be discussed in detail in Sections 3.6 and 3.7.

Some experiments with Pd–Pt/MSA catalysts were intentionally carried out up to almost total 4,6-DMDBT conversion and the corresponding selectivities and residual S contents are given in Table 6. The overwhelming product was always DMBCH while TOL, MCH and MCHT were present in smaller amounts. The GC analyses showed the absence of TH-DMDBT in these mixtures. The values of residual S content determined by independent XRF analyses were in fairly good agreement with the values of x_{DMDBT} evaluated by GC. It is also apparent, that the more acidic catalysts prepared from MSA9 and MSA13 gave roughly twofold amount of the cracking products (TOL and MCH) and less DMBCH than the less acidic catalysts prepared from MSA2. It is obvious that the acidity of catalysts controlled the composition of the obtained hydrocarbon mixture, i.e., the HYD/cracking selectivity. The above results confirm the ability of some Pd–Pt/MSA catalysts to transform the refractory 4,6-DMDBT into S-free hydrocarbons mixture with the residual S level below 5 ppm.

In contrast to Pd–Pt/MSA catalysts, only two main products were obtained with sulfided $CoMo/Al_2O_3$ at the same experimental conditions (Table 5). MCHT and DMBP were formed by the HYD and DDS routes (Scheme 1), respectively, in accordance with the literature [1,20,21,28]. TOL and MCH were detected only in trace amounts as can be expected because of much lower acidity of $CoMo/Al_2O_3$ [29]. The second difference was a much lower activity of the conventional catalyst compared to Pd–Pt/MSA catalysts. Surprisingly, two Pd–Pt samples with the lowest metal loadings close to 0.10 wt.% were still 5–7 times more active than the weight equivalent of $CoMo/Al_2O_3$.

3.5. *Effect of metal loading on acidity of Pd–Pt/MSA catalysts*

The activity of MSA supports and Pd–Pt/MSA catalysts in cumene cracking is shown as a function of metal loading in Fig. 5. It is interesting that the deposition of both metals led to progressive increase of cumene conversions x_{CU} by 10–30%. The acidities of the catalysts were therefore higher than the acidities of their supports and moreover, they decreased in the same order as those for supports: Pd–Pt/MSA9 > Pd–Pt/MSA13 > Pd–Pt/MSA4 > Pd–Pt/MSA2. This interesting result is in agreement with some recent studies showing that Pt and Pd often modify the acidity of silica–alumina based supports. In some cases, deposition of 0.8% Pd on ZSM-5 and Beta zeolites have practically no influence [30] while in the others the addition of 2% Pt to mordenite, Beta and MCM-41 led to some reduction of the strongest Brønsted sites and to increase of the sites with the medium acid strength. This was explained by the formation of the new protonic sites during the impregnation process [31]. In the case of ASA, deposition of 0.3–0.6% Pd led to a maximum of medium Brønsted acidity and was ascribed to the polarization of the OH bond by metal particles [32]. Similar effect was observed in another study after addition of 0.06–1.2% Pt to ASA [33]. In the present work, positive effects of Pd and Pt phase on

Table 6
Selectivity of reaction and residual S content at almost total 4,6-DMDBT conversion. 300 °C, 5 MPa.

Catalyst	W (mg)	F_{DMDBT} (mmol/h)	x_{DMDBT}	Selectivity (%)				S content[b] (ppm)
				MCHT	TOL	MCH	DMBCH[a]	
0.10PdPt/MSA2	22.9	0.048	0.996	0	6	12	82	2.3
0.32PdPt/MSA2	17.7	0.102	0.97	4	5	8	83	18.5
0.74PdPt/MSA13	75.2	0.272	1.00	7	14	15	64	0.4
PdA–PtO	35.1	0.136	1.00	6	13	14	67	0.8

[a] Mixture of isomers, calculated as balance.
[b] Determined in reaction mixture by XRF.

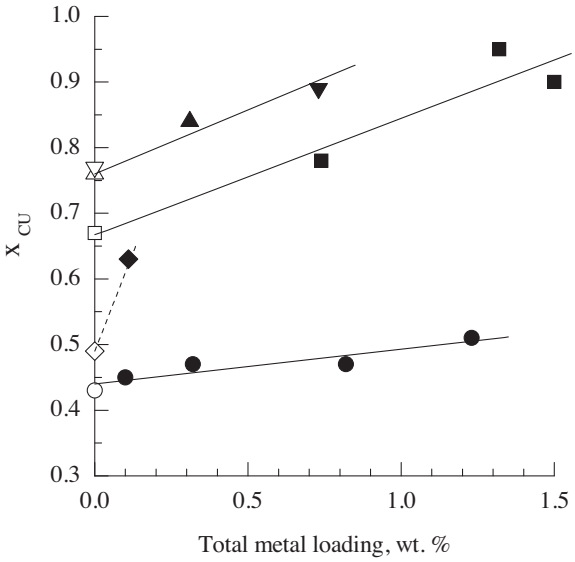

Fig. 5. Conversion of cumene cracking x_{CU} as a function of total metal loading. PdPt/MSA2 (●), PdPt/MSA4 (♦), PdA–PtO (▼), PdPt/MSA9 (▲), PdPt/MSA13 (■). Open points for supports: MSA9 from Ref. [15] (▽), new batch of MSA9 (△).

Brønsted acidity of MSA were also achieved, although their origin is not yet known. Besides of the explanations given above, possibly also creation of the new protonic sites by hydrogen activated on metallic sites and migrating to Al—O—Si sites of MSA can occur.

3.6. *Effect of metal loading on HDS activity of Pd–Pt/MSA catalysts*

The influence of the metal loading on HDS activity is shown in Fig. 6. A brief look on the whole data set reveals an increasing trend with some fluctuations which may most likely arise from different composition of the supports. Within the catalysts prepared from the same support, MSA2, the dependence is smooth and strongly non-linear. The k_{DMDBT} values increased with the metal loading up to around 0.3 wt.% and then their increment diminished. The same seems to hold for 0.31PdPt/MSA9 and PdA–PtO, both prepared from MSA9. Such non-linear dependence could mean a lower utilization of the active phase above 0.3 wt.% metal on the supports with lower Al_2O_3 content. On the other hand, almost proportional increase of activity was observed on the Pd–Pt/MSA13 samples after approximately twofold increase of the metal content 0.74 wt.%. The data in Fig. 6 show that the effect of metal amount on activity is greatly influenced by the content of Al_2O_3 in MSA.

Generally, amorphous silica–alumina consists of domains of the mixed silica–alumina phase and separate zones of SiO_2 and Al_2O_3 clusters [22]. It can be assumed that MSA13 contains the greatest fraction of the separate Al_2O_3 domains while MSA2 would be in this respect deficient. It is likely that certain fraction of Al_2O_3 in MSA serves as a preferential adsorption matrix both for the metal precursors during catalysts preparation and for the reactant molecules in the reaction. This assumption is supported by earlier findings showing that $PdCl_2$ and H_2PtCl_6 adsorb strongly on alumina [34,35] while weakly or practically not on silica [35–37]. At the same time, Aparicio et al. recently showed that the adsorption of 4,6-DMDBT on γ-Al_2O_3 was approximately 50 times higher than adsorption on SiO_2 with comparable surface area [38]. We therefore speculate that different adsorption of 4,6-DMDBT can also be expected on our catalysts prepared from MSA with different Al_2O_3 contents. The logical consequence is that this adsorption and consequently HDS reaction will be limited at higher metal loadings on the catalysts prepared from the more extracted MSA such as MSA2. These catalysts obviously suffer from deficiency of the free Al_2O_3 surface needed in the reaction, which was already exhausted by deposition of the metals. On the other hand, it seems that MSA13 has obviously some reserve in the capacity to accommodate both the metals as well as 4,6-DMDBT which allows an almost proportional increase of activity up to loading 1.50 wt.% or maybe even higher. However, data in Fig. 6 show that the most effective metal loading with the best HDS performance/metal amount ratio was found between 0.10–0.30 wt.% metal on MSA2 and MSA4. This is important from practical point of view, taking into account the price of both metals.

As far as the effect of metal dispersion on HDS activity is concerned, we failed to observe any trend between k_{DMDBT} calculated per mol of metals and H/(Pd + Pt) ratios (not shown). This is the result similar to those observed earlier in HDS of 4,6-DMDBT for Pt and Pd of different dispersions deposited on mesoporous NaH-ZSM-5, NaH-ZSM-5 and Al_2O_3 by Sun et al. [10] and in HDS of DBT

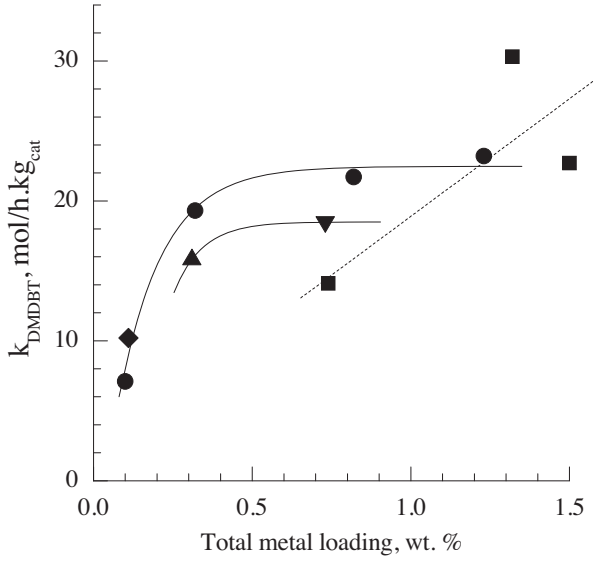

Fig. 6. First-order rate constant for 4,6-DMDBT disappearance as a function of total metal loading. PdPt/MSA2 (●), PdPt/MSA4 (♦), PdA–PtO (▼), PdPt/MSA9 (▲), PdPt/MSA13 (■).

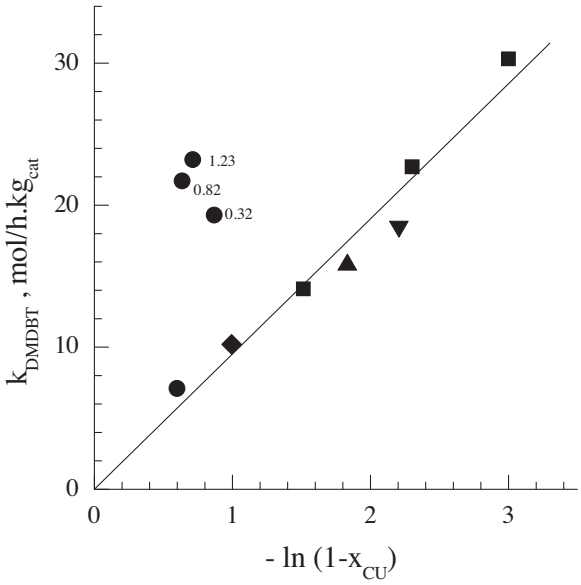

Fig. 7. Correlation between activity of Pd–Pt catalysts in HDS of 4,6-DMDBT and cumene cracking. PdPt/MSA2 (●), PdPt/MSA4 (♦), PdA–PtO (▼), PdPt/MSA9 (▲), PdPt/MSA13(■). The values near to symbols give total metal loading.

over series of Pd–Pt/Al_2O_3 catalysts [39]. In our case, the main reason is most likely the complexity of 4,6-DMDBT transformation involving several steps with different requirements to this parameter. HYD of aromatic ring, which is dominating reaction route in our case, is generally facilitated by larger ensembles of the metallic sites, i.e., by the lower metal dispersion, while the following C—S bond cleavage proceeds more easily on the sites with the higher dispersion [7]. Such situation makes difficult to obtain straightforward conclusions for 4,6-DMDBT reaction as a whole.

3.7. Acidity and HDS activity of Pd–Pt/MSA

In attempt to better understand the relation between HDS activity and acidity of catalysts, the rate constants k_{DMDBT} were plotted against the values $-\ln(1-x_{CU})$, proportional to the first-order rate constants of cumene cracking. Fig. 7 shows that a satisfactory correlation was observed with seven catalysts, confirming that their acidity plays in 4,6-DMDBT transformation an important role. As can be expected, the most active samples of this group (1.32PdPt/MSA13, 1.50PdPt/MSA13, PdA–PtO, 0.31PdPt/MSA9 and 0.74PdPt/MSA13) were prepared from the most acidic supports and the less active catalysts (0.11PdPt/MSA4 and 0.10PdPt/MSA2) from the less acidic supports. On the other hand, three experimental points for the samples prepared from MSA2 markedly deviated from this correlation. These catalysts showed still surprisingly high activities which can be ascribed exclusively to their higher metal contents.

It can be speculated that within the MSA2 supported samples their acidity can play a major role only for those with low metal loadings. This is the case of 0.10PdPt/MSA2, where contribution of the effect of metal to the overall activity is either too low or more or less balanced with acidity so its effect becomes apparent and therefore, this sample falls into correlation. The metal loadings of the remaining three samples are substantially higher, leading to the overwhelming effect of the metals and to only marginal or even none effect of acidity. This assumption suggests that the low acidity of these samples could be an additional factor limiting the HDS activity of MSA2 supported catalysts at the loadings above 0.3 wt.% metal.

The above results documenting the importance of acidity of Pd–Pt/MSA catalysts in HDS of 4,6-DMDBT are in accordance with the recent observations of other researchers that combination of acidity and mesoporosity substantially improves HDS of 4,6-DMDBT on Pd, Pt and Pd–Pt on mesoporous zeolites such as NaH-ZSM-5 [10], Pd on mesoporous Y, Beta and ZSM-5 [11] and Pd on mesoporous USY [12]. As far as the mesoporosity of MSA is concerned, we believe it also contributes to the superior HDS activity of Pd–Pt catalysts. Their pore size around 4 nm is close to the value 4.9 nm for mesoporous Na-ZSM-5 which gave the highly active Pd–Pt catalysts [9]. Moreover, it was reported that 4,6-DMDBT molecule with the size similar to microporosity of Pd/Y 0.74×1.3 nm can also be transformed by HDS, although with a lower velocity as compared to its mesoporous Pd/Y counterpart [11]. Taking into account these considerations and the high activity of Pd–Pt/MSA catalysts, it seems that their pore size does not represent a major problem concerning the diffusion and reaction of 4,6-DMDBT molecule inside the catalyst particles.

It can finally be concluded, that the amount of Al_2O_3 phase in MSA supports has multiple effect on the activity and selectivity of Pd–Pt catalysts. It controls the Brønsted acidity of the supports and catalysts, the amount of deposited active metal phase and consequently the overall HDS activity and HYD/cracking selectivity of catalysts. Moreover, it is anticipated that the low content of Al_2O_3 could also limit the adsorption of 4,6-DMDBT during reaction and due to lower Brønsted acidity weaken the cooperation with the metal phase at loadings above 0.3 wt.%.

4. Conclusions

Mesoporous silica–aluminas (MSA) containing 2–13 wt.% Al_2O_3 showed promising properties as supports of Pd–Pt catalysts for HDS of 4,6-DMDBT. Four MSA supports showed the surface areas 385–611 m^2/g, high mesoporosity and Brønsted acidity. They transformed refractory 4,6-DMDBT at 300 °C by isomerization and disproportionation into more reactive 3,6-DMDBT, 4-MDBT and TMDBT. HDS on Pd–Pt/MSA catalysts proceeded almost exclusively by the HYD route and increased with the metal loading. This dependence was affected by the content of Al_2O_3 phase in MSA. It was strongly non-linear for the catalysts prepared from the MSA with the lowest Al_2O_3 content of 2 wt.% while almost proportional for those containing 13 wt.% Al_2O_3. The most effective catalysts, in the sense of HDS performance per noble metal amount, were those with 0.10–0.30 wt.% metal on the MSA containing 2 and 4 wt.% Al_2O_3. All Pd–Pt catalysts were generally much more active than the conventional catalyst. The most interesting new finding is that the lowest metal loadings around 0.10 wt.% on MSA gave still 5–7 time more active catalysts than sulfided CoMo/Al_2O_3. Activities of the majority of Pd–Pt catalysts correlated with their Brønsted acidities while not with metal dispersion. The amount of Al_2O_3 phase in the support had several effects on the properties of Pd–PtPd–Pt catalysts. It controlled their Brønsted acidity, amount of the deposited metal phase including their mutual interaction, which finally contributed to the overall HDS activity and HYD/cracking selectivity. Low loaded noble metal catalysts prepared from the modified MSA supports could be useful in the second-stage HDS for effective removal of the most refractory S compounds.

Acknowledgement

The financial support of the Czech Science Foundation, Czech Republic (grant P106/11/0902) is gratefully acknowledged. The authors thank to J. Karban for GC–MS analyses of some reaction products.

References

[1] T. Isoda, S. Nagao, X. Ma, Y. Korai, I. Mochida, Energy Fuels 10 (1996) 1078–1082.
[2] F. Richard, T. Boita, G. Pérot, Appl. Catal. A 320 (2007) 69–79.
[3] P. Michaud, J.L. Lemberton, G. Pérot, Appl. Catal. A 169 (1998) 343–353.
[4] T. Isoda, Y. Takase, K. Kusakabe, S. Morooka, Energy Fuels 14 (2000) 585–590.
[5] S.K. Bej, S.K. Maity, U.T. Turaga, Energy & Fuels, ACS J. 18 (5) (2004) 1227–1237.
[6] H.R. Reinhoudt, R. Troost, A.D. van Langeveld, S.T. Sie, J.A.R. van Veen, J.A. Moulijn, Fuel Process. Technol. 61 (1999) 133–147.
[7] A. Niquille-Röthlisberger, R. Prins, Catal. Today 123 (2007) 198–207.
[8] Y. Yoshimura, M. Toba, T. Matsui, M. Harada, Y. Ichihashi, K.K. Bando, H. Yasuda, H. Ishihara, Y. Morita, T. Kameoka, Appl. Catal. A 322 (2007) 152–171.
[9] Y. Sun, R. Prins, Angew. Chem. Int. Ed. 47 (2008) 8478–8481.
[10] Y. Sun, H. Wang, R. Prins, Catal Today 150 (2010) 213–217.
[11] W. Fu, L. Zhang, T. Tang, Q. Ke, S. Wang, J. Hu, G. Fang, J. Li, F. Xiao, J. Am. Chem. Soc. 133 (2011) 15346–15349.
[12] L. Zhang, W. Fu, Q. Ke, S. Zhang, H. Jin, J. Hu, S. Wang, T. Tang, Appl. Catal. A 433–434 (2012) 251–257.
[13] Z. Vít, O. Šolcová, Micropor. Mesopor. Mater. 96 (2006) 197–204.
[14] Z. Vít, D. Gulková, L. Kaluža, S. Bakardieva, M. Boaro, Appl. Catal. B 100 (2010) 463–471.
[15] Z. Vít, H. Kmentová, L. Kaluža, D. Gulková, M. Boaro, Appl. Catal. B 108–109 (2011) 152–160.
[16] Z. Vít, D. Gulková, L. Kaluža, M. Boaro, Appl. Catal. B 146 (2014) 213–220.
[17] A. Corma, B.W. Wojciechowski, Catal. Rev. - Sci. Eng. 24 (1) (1982) 1–65.
[18] Z. Vít, D. Gulková, L. Kaluža, M. Zdražil, J. Catal. 232 (2005) 447–455.
[19] J.R. Anderson, K.C. Pratt, Introduction to Characterization and Testing of Catalysts, Academic Press (Harcourt Brace Jovanovish, Publishers), New York, 1985, p. 64.
[20] Ch. Kwak, J.J. Lee, J.S. Bae, S.H. Moon, Appl. Catal. B 35 (2001) 59–68.
[21] J.H. Kim, X. Ma, C. Song, Y. Lee, S.T. Oyama, Energy Fuels 19 (2005) 353–364.
[22] G. Crépeau, V. Montouillout, A. Vimont, L. Mariey, T. Cseri, F. Maugé, J. Phys. Chem. B 110 (2006) 15172–15185.
[23] T.B. Flanagan, J.D. Clewley, H. Noh, J. Barker, Y. Sakamoto, Acta Materialia 46 (6) (1998) 2173–2183.
[24] Y. Yu, B. Fonté, A. Jentys, G.L. Haller, J.A.R. van Veen, O.Y. Gutiérrez, J.A. Lercher, J. Catal. 292 (2012) 1–12.
[25] Y. Yu, O.Y. Gutiérrez, G.L. Haller, R. Colby, B. Kabius, J.A.R. van Veen, A. Jentys, J.A. Lercher, J. Catal. 304 (2013) 135–148.
[26] R. Roldán, A.M. Beale, M. Sánchez-Sánchez, F.J. Romero-Salguero, C. Jiménez-Sanchidrián, G. Gómez, J. Catal. 254 (2008) 12–26.
[27] U. Nylén, J.F. Delgado, S. Järås, M. Boutonnet, Fuel Process. Technol. 86 (2004) 223–234.
[28] N. Hermann, M. Brorson, H. Topsøe, Catal. Lett. 65 (2000) 169–174.
[29] E. Lecrenay, K. Sakanishi, I. Mochida, Catal. Today 39 (1997) 13–20.
[30] F. Dorado, R. Romero, P. Cañizares, Appl. Catal. A 236 (2002) 235–243.
[31] D. Kubička, N. Kumar, T. Venäläinen, H. Karhu, I. Kubičková, H. Österholm, D.Y. Murzin, J. Phys. Chem. B 110 (2006) 4937–4946.
[32] F. Regali, L.F. Liotta, A.M. Venezia, V. Montes, M. Boutonnet, S. Järås, Catal. Today 223 (2014) 87–96.
[33] F. Regali, L.F. Liotta, A.M. Venezia, M. Boutonnet, S. Järås, Appl. Catal. A 469 (2014) 328–339.
[34] P.S.S. Reddy, N.S. Babu, N. Lingaiah, P.S.S. Prasad, I.V. Rao, Proc. of Europ. Congr. of Chem. Eng. (ECCE-6), Abstr. No. 777, Copenhagen, 16-20 September 2007. http://www.nt.ntnu.no/users/skoge/prost/proceedings/ecce6_sep07/upload/777.pdf.
[35] T. Mang, B. Breitscheidel, P. Polanek, H. Knözinger, Appl. Catal. A 106 (1993) 239–258.
[36] K.M.E. Attyia, N.E. Fouad, J. Therm. Anal. 42 (1994) 1207–1219.
[37] J.T. Miller, M. Schreier, A.J. Kropf, J.R. Regalbuto, J. Catal. 225 (2004) 203–212.
[38] F. Aparicio, E. Camú, M. Villarroel, N. Escalona, P. Baeza, J. Chil. Chem. Soc. 58 (4) (2013) 2057–2060.
[39] V.G. Baldovino-Medrano, P. Eloy, E.M. Gaigneaux, S.A. Giraldo, A. Centeno, J. Catal. 267 (2009) 129–139.